JACS
JOURNAL OF THE AMERICAN CHEMICAL SOCIETY

ARTICLE

pubs.acs.org/JACS

Thermodynamics of Supramolecular Naphthalenediimide Nanotube Formation: The Influence of Solvents, Side Chains, and Guest Templates

Nandhini Ponnuswamy,[†] G. Dan Pantoş,*[,†,‡] Maarten M. J. Smulders,[†] and Jeremy K. M. Sanders*[,†]

[†]University Chemical Laboratory, University of Cambridge, Lensfield Road, Cambridge CB2 1EW, United Kingdom

[‡]Department of Chemistry, University of Bath, Bath BA2 7AY, United Kingdom

Supporting Information

ABSTRACT: Amino-acid functionalized naphthalenediimides self-assemble into hydrogen-bonded supramolecular helical nanotubes via a noncooperative, isodesmic process; the self-assembly of ordered helical systems is usually realized through a cooperative process. This unexpected behavior was rationalized as a manifestation of entropy−enthalpy compensation. Fundamental insights into the thermodynamics governing this self-assembly were obtained through the fitting of the isodesmic model to ^{1}H NMR spectrometry and circular dichroism spectroscopy measurements. Furthermore, we have extended the application of this mathematical model, for the first time, to quantitatively estimate the effect of guests, solvents, and side chains on the stability of the supramolecular nanotube; most significantly, we demonstrate that C_{60} acts as a template to stabilize the nanotube assembly and thereby substantially increase the degree of polymerization.

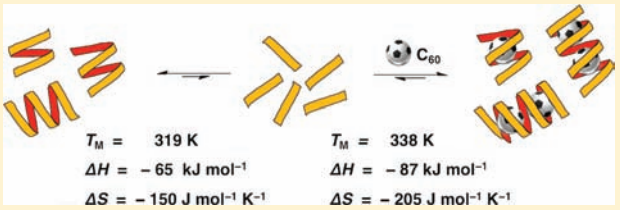

INTRODUCTION

We describe here the thermodynamics governing the self-assembly of amino-acid functionalized naphthalenediimide (NDI) supramolecular helical nanotubes in $CHCl_3$ and 1,1,2,2,-tetrachloroethane (TCE) solutions. We have used mathematical models for supramolecular polymerizations to show that, contrary to our expectation, the supramolecular polymerization of NDI helical nanotubes occurs via a non−cooperative, isodesmic mechanism. We have calculated the association constants leading to the formation of the supramolecular nanotube and, for the first time, have extended the application of the isodesmic model to quantify the effect of stabilizing and destabilizing guests, solvents and side chains on the stability of the nanotube. A surprising role for entropy−enthalpy compensation in nanotube formation is also discussed.

The self-assembly of a quasi-one-dimensional supramolecular polymer is described either via an isodesmic or a cooperative mechanism.[1−5] In an isodesmic mechanism, the addition of each monomer to the growing chain is governed by a single equilibrium constant, K_e. This implies that there is a broad distribution in the degree of polymerization, with substantial numbers of long objects being only obtained either at high concentrations or low temperatures, or for high association constants. In contrast, the cooperative mechanism is characterized by an activation step, governed by equilibrium constant, K_2, which precedes chain elongation with equilibrium constant K_e. If $K_2 \ll K_e$, the polymerization becomes cooperative and is reminiscent of an actual phase transition. This implies a sharp change in the degree of aggregation above which there is enhanced propensity for monomer addition to the growing chain. The formation of chiral, helical supramolecular structures is often associated with a cooperative growth mechanism as the number of interactions between individual monomer units increases when the first turn of the helix is closed.[4] Cooperative helical systems have been reported previously in biological polymers, with notable examples being the nucleated formation of actin[6−8] and tubulin.[9] Some synthetic examples of such systems include the supramolecular polymerization of perylenediimide chromophores,[10] amphiphilic hexa-*peri*-hexabenzocoronenes,[11,12] cyclotriveratrylene derivatives equipped with dendrons,[13,14] dendronized dipeptides[15] and oligo(*p*-phenylene vinylenes) equipped with ureidotriazine self-complementary quadruple hydrogen bonding units.[16,17]

Previously, we have reported that amino-acid functionalized NDIs form supramolecular nanotubes (diameter =12.4 Å) in aprotic solvents of medium polarity such as $CHCl_3$ and TCE: the monomers are held together by COOH hydrogen-bonded dimerization between the *i* and *i* + 1 monomers and also by non−classical CH···O hydrogen bonds between the *i* and *i* + 3 monomers.[18] These nanotubes have been characterized by circular dichroism and X-ray diffraction methods (Figure 1) and were found to act as receptors for fullerenes,[19,20] condensed aromatic systems,[21] and quaternary ammonium ions.[22] To date, we have only reported a qualitative description of the binding events in the formation of the nanotube and host−guest complexes: these have been difficult systems to study due to the unknown length

Received: September 26, 2011
Published: November 18, 2011

ACS Publications © 2011 American Chemical Society

dx.doi.org/10.1021/ja2088647 | *J. Am. Chem. Soc.* 2012, 134, 566–573

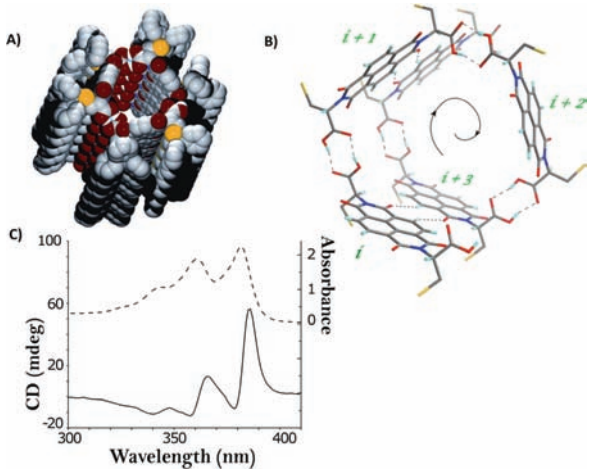

Figure 1. (A) Space-filling and (B) stick-representation highlighting the H-bonding pattern (dashed lines) of the X-ray structure of **1a** obtained from CH_2Cl_2; the trityl groups have been removed for clarity. (Color scheme: gray, C; cyan, H; red, O; blue, N; yellow, S). (C) Absorption (dashed line) and CD (solid line) spectra of a 5.0×10^{-4} M solution of **1a** in $CHCl_3$.

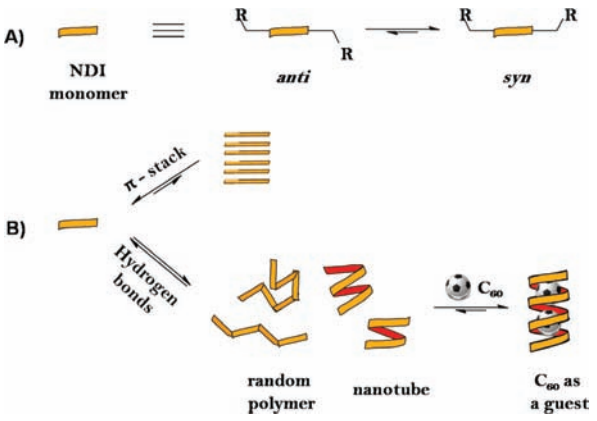

Figure 2. Schematic representation of the equilibria between (A) *anti* and *syn* side chain conformations of the NDI monomer and (B) possible NDI aggregates in $CHCl_3$ or TCE solution.

distribution of the nanotube host, the undefined stoichiometry of the interaction with guests, and the low chloroform solubility of C_{60}. However, recent developments in the analysis of self-assembly mechanisms of supramolecular polymerizations have allowed us to investigate the mechanism of formation of the NDI nanotubes and quantitatively estimate the effect of host−guest interactions.[1−5]

RESULTS AND DISCUSSION

Thermodynamics of the Formation of the Nanotube. In order to investigate the relative stability of amino-acid functionalized NDI supramolecular nanotubes, we considered all possible supramolecular NDI aggregates present in solution as being in equilibrium with each other (Figure 2). This equilibrium is effectively a dynamic combinatorial library[23−26] in which the NDI building blocks are connected through reversible hydrogen bonds to give a mixture of species under thermodynamic control.

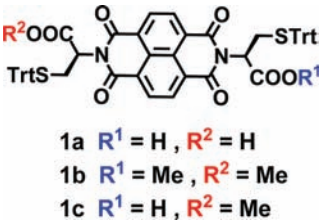

Figure 3. Amino-acid functionalized NDIs used in this study.

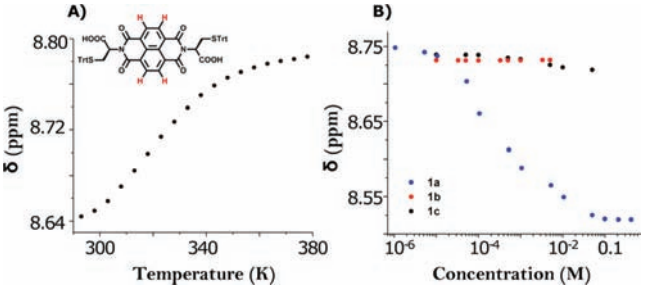

Figure 4. (A) Effect of temperature on the chemical shift of the NDI protons; [**1a**] = 0.9×10^{-3} M in TCE. (B) Concentration-dependent chemical shift of the NDI protons of **1a** (blue dots), **1b** (red dots), and **1c** (black dots) at 300 K in $CHCl_3$.

S-trityl protected cysteine functionalized NDIs **1**(**a**−**c**) were chosen for this study due to their enhanced solubility in chlorinated solvents compared to other amino-acid functionalized NDIs (Figure 3).

The side chains of the NDI monomer can be arranged in the *syn* or the *anti* conformation with respect to the naphthalene core (Figure 2a). The consideration of *syn*−*anti* equilibrium is relevant because the NDI nanotube can only form through the hydrogen-bonded self-assembly of *syn* conformers. X−ray diffraction of crystals of **1**(**a**,**b**) grown from solvents of differing polarities and molecular modeling studies have shown that the *syn* conformer is unexpectedly preferred over the *anti* conformer in chlorinated solvents, presumably due to favorable side chain interactions (see SI).

The NDI monomer might be expected to aggregate via π-stacking and/or hydrogen bonds.[27,28] In $CHCl_3$, the formation of π-stacked polymers is unfavorable on both electronic and steric grounds: NDI has an electron deficient aromatic core and the association constant for the stacking of two NDI units in $CHCl_3$ has been reported by Iverson and Cubberley to be less than 1 M^{-1}.[29] Additionally, the steric hindrance provided by the amino acid side chains destabilizes the formation of any aggregate formed by $\pi-\pi$ interactions. Thus, the formation of supramolecular polymers by π-stacking of NDI units can be safely ignored when considering the possible equilibria of NDIs in solution. With respect to hydrogen-bonded structures, both NDI conformers can self-assemble via COOH dimerization to form a random supramolecular polymer, but only the poly-*syn*-NDI can further fold to form the supramolecular nanotube (Figure 2b).

Concentration- and temperature-dependent ^{1}H NMR experiments were performed to gain insight into the self-assembly of **1a** in solution. The single NDI resonance around 8.6 ppm (from the aromatic protons shown in red in Figure 4) in ^{1}H NMR spectra (500 MHz) of compound **1a** dissolved in $CHCl_3$ or TCE is highly dependent on both concentration and temperature.

dx.doi.org/10.1021/ja2088647 |J. Am. Chem. Soc. 2012, 134, 566–573

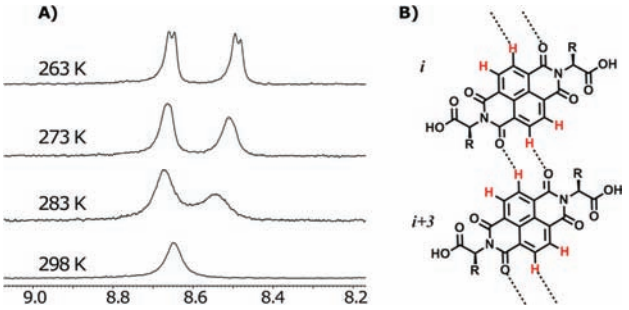

Figure 5. (A) ^{1}H NMR spectrum of the NDI aromatic protons (shown in red) of a 0.9×10^{-3} M solution of **1a** in TCE at different temperatures. (B) CH···O hydrogen-bonding between NDI *i* and *i* + 3 in the nanotube, as observed in the crystal structure.

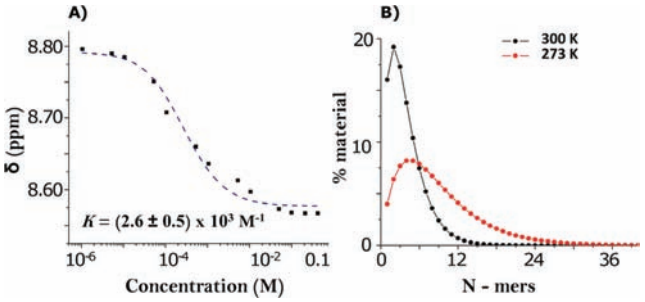

Figure 6. (A) Isodesmic fit of the concentration-dependent ^{1}H NMR chemical shift of **1a** at 300 K in $CHCl_3$. (B) Calculated distribution of material over different nanotube lengths (number of aggregated monomers, in short *N*-mers) at 300 K (black trace) and 273 K (red trace).

This resonance becomes more shielded by around 0.15 ppm on decreasing the temperature (from 378 to 293 K, Figure 4a) and by around 0.25 ppm on increasing the concentration (from 1.0×10^{-6} M to 0.7 M, Figure 4b, blue dots). Significantly smaller shifts (less than 0.03 ppm) in this proton resonance were observed in **1b**, which cannot form hydrogen bonds (Figure 4b, red dots) and in monotopic derivative **1c** which can only form a hydrogen-bonded dimer (Figure 4b, black dots). These observations are in accordance with **1a** forming a higher order, hydrogen-bonded supramolecular structure in solution.

Lowering the sample temperature below 298 K results in splitting of the broad singlet at 8.6 ppm into two peaks, which further resolve into doublets at temperatures below 265 K as shown in Figure 5a. The splitting of the NDI peak at lower temperatures supports the idea that NDIs predominantly form a well-defined and well-ordered hydrogen-bonded supramolecular structure with two different environments for the NDI protons. This is entirely consistent with the repetitive arrangement of NDI building blocks held as a nanotube, as shown in Figure 5b. In a random hydrogen-bonded polymer (see Figure 2), the NDI aromatic protons should experience an effectively symmetric environment and consequently appear as a singlet in the ^{1}H NMR spectrum; by contrast, in the nanotube, the geometry imposed by the proposed additional C−H···O hydrogen bonds desymmetrizes the NDI aromatic protons by placing them in different chemical environments, resulting in the splitting of their ^{1}H resonances. Lowering the temperature slows down the exchange between the nonaggregated NDI monomers and those in a nanotube, thus providing a window on the dynamics of nanotube formation in solution.

The C−H···O hydrogen bonds also place the aromatic proton of the *i* NDI unit in the carbonyl shielding region[30] of the *i* + 3 NDI unit (Figure 5b). Since the observed NDI chemical shift is an average of the chemical shift of the NDI monomer, random polymer, and the nanotube, an increase in the proportion of material present as nanotubes, either at high concentrations or low temperatures, results in the shielding of the NDI aromatic proton. The very small upfield shift observed in **1c** is probably due to the formation of a hydrogen-bonded dimer.

The dependence of the chemical shift of the NDI aromatic protons on concentration was analyzed in order to shed light on the thermodynamics of nanotube formation. A smooth sigmoidal curve devoid of any sharp slope changes, suggestive of an isodesmic self-assembly mechanism, was observed in the plot of the ^{1}H NMR resonance for the NDI aromatic proton of **1a** in $CHCl_3$ at 300 K at different concentrations (Figure 4b, blue dots).[10]

For further evidence of an isodesmic mechanism, the self-association of **1a** was also studied using a Dil plot[31] developed by Hunter and Anderson, which provides a more accurate analysis for dilution experiments. In a Dil plot, the concentration switching window c_R, defined as the factorial increase in ligand concentration required to change the bound/free receptor ratio from 1:10 to 10:1, can be used as a macroscopic measure of cooperativity.[32] In other words, c_R is a measure of the sharpness of the bound−free transition. A value of log c_R = 3 represents isodesmic behavior and any deviation from this value indicates cooperativity. Fitting of the concentration-dependent ^{1}H NMR shifts of **1a** to the Dil plot gave the value of log c_R = 3.06, which confirmed that the self−association of **1a** is dominated by the isodesmic mechanism (see SI). Fitting of the above data to an isodesmic model afforded an association constant, $K = (2.6 \pm 0.5) \times 10^3$ M^{-1} for the formation of nanotubes of **1a** at 300 K (Figure 6a) in $CHCl_3$ (see SI for fitting).

The association constant for the formation of the nanotube was also calculated using concentration-dependent circular dichroism (CD) spectroscopy. The NDI monomer has a very low intrinsic CD signal, but upon forming the nanotube in $CHCl_3$ the CD signal (λ_{max} at 381 nm) intensifies dramatically. The intensity of the CD signal is therefore proportional to the proportion of NDI monomers held in the nanotubular aggregate.[33] An isodesmic fit of a plot of the CD intensity vs concentration yielded the association constant for the formation of the nanotube, in qualitative agreement with that obtained by the ^{1}H NMR method described above. However, due to technical constraints, concentrations only up to 1.0×10^{-3} M were accessible with this technique and as a result the fitting of the data was less precise ($K = (4.3 \pm 1.2) \times 10^3$ M^{-1} at 300 K; see SI).

The temperature-dependent ^{1}H NMR experiments using an automated variable temperature NMR program are more accurate and require less material than the concentration-dependent ^{1}H NMR experiments.[5] These experiments were carried out in TCE (a solvent comparable to $CHCl_3$ in terms of its hydrogen bonding abilities), allowing experiments at higher temperatures. The data obtained from the temperature-dependent ^{1}H NMR (Figure 4a) also revealed an isodesmic self-assembly mechanism for **1a** and yielded an association constant for the formation of nanotube $K = (2.9 \pm 0.02) \times 10^3$ M^{-1} at 300 K. The analysis also provided the melting temperature (where the degree of aggregation is equal to 0.5) of the nanotube T_M = 320 K, the molar enthalpy of nanotube formation $\Delta H = -65$ kJ mol^{-1} and change in entropy $\Delta S = -150$ J mol^{-1} K^{-1}, for a solution of 0.9×10^{-3} M. The association constant obtained from the temperature-dependent

dx.doi.org/10.1021/ja2088647 |J. Am. Chem. Soc. 2012, 134, 566–573

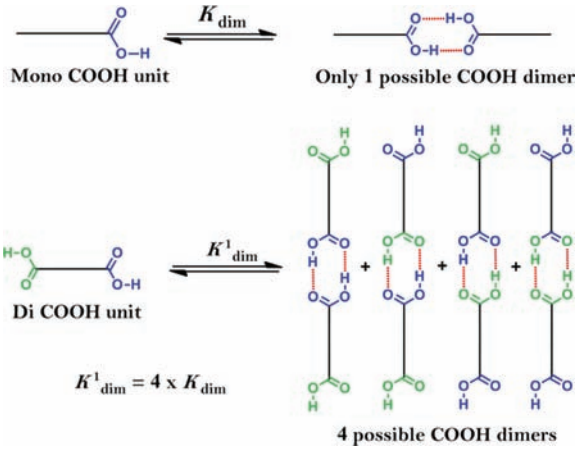

Figure 7. Schematic representation of the effect of mono- and di-COOH units on association constant (K_{dim} and K^1_{dim} respectively) of COOH hydrogen-bonded dimerization.

analysis is very close to that obtained from concentration-dependent analysis, and is experimentally much easier to obtain; this establishes the utility of temperature-dependent ^{1}H NMR to calculate association constants for this type of hydrogen-bonded system.[5] The enthalpy and entropy contributions to the Gibbs free energy changes for aggregation show that formation of the nanotube is enthalpy driven and entropically disfavored. This is expected, given that nanotube formation depends on hydrogen bonds between NDI monomers that greatly restrict conformational freedom.

The number average degree of polymerization DP_N according to the temperature-dependent isodesmic model was calculated as 5.3 at 273 K and 2.2 at 300 K for a solution of **1a** of 0.9×10^{-3} M in TCE. A simulation of the exponential distribution[7] of species in a 0.9×10^{-3} M solution with the above DP_N values showed that, at 273 K, nanotubes up to 9 helical turns, corresponding to 28 aggregated NDI monomers, were present in the solution, albeit at low concentrations (Figure 6b, see SI).

In a further exploration of the growth mechanism, we compared the dimerization constant of COOH hydrogen bonds in the NDI monomer to the equilibrium constant for the formation of the nanotube, which should be similar in an ideal isodesmic system. To estimate the dimerization constant for the formation of COOH hydrogen-bonded dimers, a two state monomer–dimer binding model was used to fit the concentration-dependent ^{1}H NMR data of monotopic molecule **1c**. A value of $(2.1 \pm 0.2) \times 10^2$ M^{-1} was obtained at 300 K, which is an order of magnitude lower than the equilibrium constant for the formation of nanotube of **1a**.[34] Much of the large apparent difference in association constant obtained for **1c** and **1a** can be accounted for by a statistical factor of 4 that distinguishes association of a molecule containing one (**1c**) vs two (**1a**) COOH functional groups as illustrated in Figure 7. Considering this factor of 4 in the dimerization constant renders the cooperativity present in molecule **1a** to be only $\sigma = K_{dimer}/K_{nanotube} = 0.48$, which is probably too small to be observed experimentally and thus the experimental data fits closely to an isodesmic mechanism (simulated graph in SI).

The conclusion that the growth of NDI nanotubes could be effectively explained by an isodesmic mechanism was unexpected, since the formation of helical structures is usually cooperative because the number of attractive interactions between monomers increases when the first turn of the helix is closed. The lack of significant cooperativity, in spite of the presence of additional interactions after the formation of one helical turn in the nanotube, is probably a manifestation of entropy–enthalpy compensation: this is the widely documented empirical observation that the increased enthalpic benefits of tighter binding generally results in increased entropic costs due to more restricted relative motion.[35−40] The two effects can cancel each other out because the energetic gain from the formation of noncovalent bonds is, at room temperature, comparable to the entropic losses that oppose them.

In the case of the NDI nanotubes, the enthalpic cooperativity obtained by the formation of additional putative CH···O hydrogen bonds between i and $i + 3$ NDI units and by interactions between the solvent and the NDI units is almost completely compensated by entropic costs due to higher ordering of the side chains, as a result of which no significant cooperativity in free energy is observed (see SI).

Having elucidated the mechanism of formation of NDI nanotubes, we then applied the isodesmic model to explore the effect of side chain interactions on the stability of the nanotube.

Effect of Side Chain Interactions on Nanotube Stability. As these nanotubes are held together primarily by hydrogen bonding between carboxylic acid groups, they can be disassembled by base-induced deprotonation.[41] Acid–base titration experiments led us to conclude that, among the amino acid derivatives we have studied, *S*-trityl protected cysteine functionalized NDIs (**1a**) formed the most stable nanotube in solution, while ε-NHBoc protected lysine (**2**) and isoleucine (**3**) functionalized NDIs formed less stable nanotubes. Molecules **2** and **3** were therefore chosen for studying the effect of side chains on the stability of the nanotube. Chirooptical studies on equimolar concentrations of **1a**, **2**, and **3** in chloroform gave a relatively higher CD signal intensity for **1a**, also suggesting that the proportion of monomer held as a nanotube was relatively higher in **1a**. These experiments gave a qualitative scale of the relative strengths of the nanotubes derived from different NDIs but failed to give a quantitative measurement or comparison of association constants for the formation of these nanotubes.

We therefore applied the above analytical approach to the variable temperature ^{1}H NMR data of **2** and **3** in order to calculate their association constants. In the case of **2**, the equilibrium in solution could be complicated since the presence of a Boc protecting group could in principle lead to the competitive formation of polymers held by CONH hydrogen bonds; however literature precedents indicate that this process is not very likely to occur.[42]

Fitting the isodesmic model to the temperature-dependent ^{1}H NMR chemical shift of the NDI aromatic proton of **2** and **3** for a 0.9×10^{-3} M and 1.0×10^{-3} M TCE solution, respectively, resulted in similar values for association constants, $K = (1.26 \pm 0.02) \times 10^3$ M^{-1} and $K = (1.09 \pm 0.06) \times 10^3$ M^{-1} at 300 K (Figure 8). The higher association constant obtained for molecule **1a** compared to **2** and **3** is in agreement with our earlier qualitative observations; this may be due to (1) differences in solvation and/or creation of a more nonpolar environment in sterically hindered **1a**, resulting in the strengthening of COOH hydrogen-bonded dimers, (2) stabilizing van der Waals' interactions between the trityl groups of i and $i + 3$ NDI units in the nanotube, (3) competition for COOH groups to form hydrogen-bonded dimers with amide groups present in the Boc side chain of **2**, and/or (4) the presence of a β-substituent in **3**, may lead to higher steric repulsions between the side chains.

dx.doi.org/10.1021/ja2088647 |J. Am. Chem. Soc. 2012, 134, 566–573

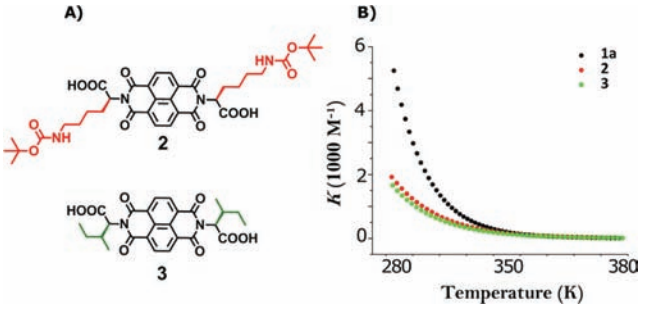

Figure 8. (A) Amino-acid functionalized NDIs used for studying the effect of side chains on the stability of the nanotube. (B) Comparison of change in association constant with temperature for **1a**, **2**, and **3**.

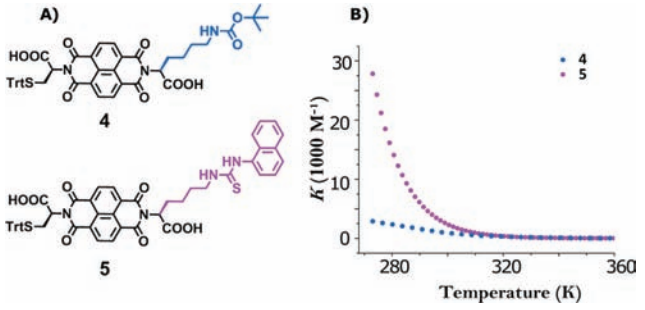

Figure 9. (A) Amino−acid functionalized NDIs used for cross−linking the side chains. (B) Comparison of the temperature-dependent association constants for **4** and **5**.

Kuroda et al. have recently shown that covalent cross-linking of a single side chain of a helical peptide can stabilize the entire helical structure.[43] Based on similar cross-linking principles, we envisaged that a thiourea functional group on the NDI side chain could result in the additional stabilization of the nanotube via additional hydrogen-bonded cross-linking of i and i + 3 NDI monomers. For this purpose, molecule **4**, which is *N*-desymmetrized with trityl protected cysteine on one side and ε-NHBoc protected lysine on the other, was synthesized using a reported literature protocol.[44,45] The Boc protecting group in molecule **4** was removed under mild acidic conditions that do not affect the trityl group. The resultant amino group was then coupled with 1-naphthyl isothiocyanate to give the desired product **5** (Figure 9a).

Chirooptical studies of molecules **4** and **5** in TCE show that both have a characteristic nanotube CD fingerprint (see SI). Comparison of the ^{1}H NMR properties of **5** with a model compound butyl−naphthyl thiourea in TCE at 300 K shows that the thiourea is hydrogen-bonded and the naphthyl protons are shielded, suggestive of a $\pi-\pi$ interaction (see SI).

The isodesmic fit of the variable temperature ^{1}H NMR data of a 1.0×10^{-3} M, TCE solution of molecule **5** resulted in $K = (14.07 \pm 0.02) \times 10^3$ M^{-1} at 280 K (Figure 9b). Comparison of the association constants for molecules **4** ($K = (4.32 \pm 0.04) \times 10^3$ M^{-1}) and **5** at 280 K shows that the nanotubes formed by molecule **5** are indeed stronger by a factor of *6*, in agreement with our expectations. However, comparing **5** with **1a** we found that the two nanotubes are characterized by similar association constants. This can be explained if the introduction of the thiourea moiety has a stabilizing effect on the nanotube formation due to intermolecular hydrogen bonds, offsetting the loss of the trityl groups which appear to have a stabilizing effect through solvophobic interaction.

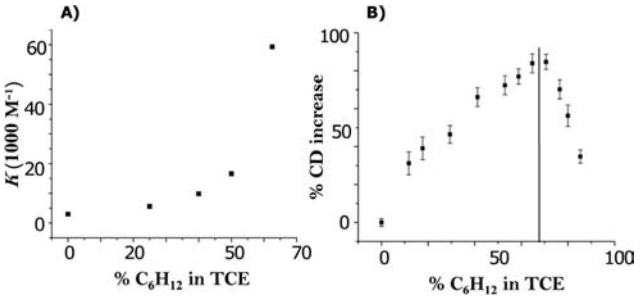

Figure 10. (A) Plot of association constant (K) for the formation of nanotube, calculated for a 1.0×10^{-3} M solution of **1a** vs the percentage of cyclohexane in TCE. (B) Plot of the CD_{max} signal intensity (mdeg) for a 1.2×10^{-4} M solution of **1a** vs the percentage of cyclohexane in TCE at 300 K (error bars with respect to error in CD intensity on multiple runs).

These results emphasize the significance of the side chain interactions in the formation of the nanotube. Nanotubes formed from **1a** containing the bulky trityl side chain are more stable than the ones derived from **2** and **3** containing an alkyl side chain, mainly due to solvophobic effects. However in the case of molecule **5** compared to **4**, the external stabilization obtained by the non−covalent cross-linking of the i and i + 3 NDI monomer through the hydrogen bonding of thiourea functional groups in the NDI side chain and via $\pi-\pi$ interactions between the naphthyl moieties, results in the enhanced stabilization of the helical core.

The solvophobic interactions leading to the superior stabilization of **1a** compared to **2** and **3** led us to investigate the role of solute−solvent interactions in the formation of the nanotube.

Effect of Solvent on the Stability of the Nanotube. Solvation is an important factor in determining the self-assembly behavior of a system. Hunter et al. have carried out in-depth investigations of the effects of solvent competition on intermolecular hydrogen bonding interactions between neutral molecules in a range of solvents.[46] Their results clearly demonstrate that in noncompetitive solvents such as cyclohexane and carbon tetrachloride, hydrogen bonds can be effectively stronger by a factor of 100 compared to partially competing solvents such as chloroform.

In order to increase the effective strength of the hydrogen bonds in the NDI nanotube, cyclohexane was added to a solution of **1a** in TCE, using CD and variable temperature ^{1}H NMR to monitor the effect (see SI). Isodesmic fitting of temperature-dependent chemical shift of the NDI aromatic proton yielded the association constant for the formation of nanotube at different ratios cyclohexane:TCE, which when plotted against the percentage of cyclohexane in TCE, showed an exponential increase in association constant with increasing amount of cyclohexane (Figure 10a). The association constant of a 1.1×10^{-3} M solution of **1a** in 6:4 cyclohexane:TCE mixture at 300 K was found to be $(59.16 \pm 0.02) \times 10^3$ M^{-1} which is 20 times higher than in pure TCE (DP_N = 8.5 vs 2.2, respectively). ^{1}H NMR experiments at higher concentrations of cyclohexane in TCE could not be performed due to the low solubility of **1a**.

The effect of cyclohexane on the strength of the nanotube was also studied using CD and UV−vis spectroscopies. The intensity of the CD signal on addition of cyclohexane to a 1.2×10^{-4} M solution of **1a** in TCE, keeping the concentration of **1a** constant, initially increases, reaching a maximum at approximately 65%

dx.doi.org/10.1021/ja2088647 |J. Am. Chem. Soc. 2012, 134, 566–573

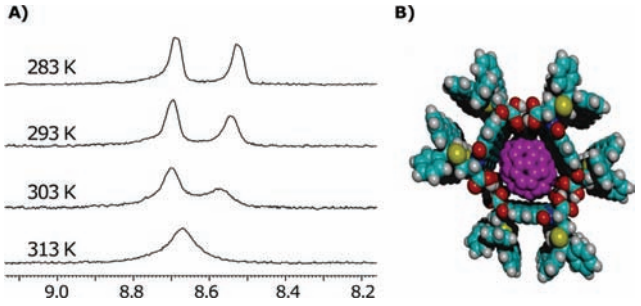

Figure 11. (A) ^{1}H NMR spectrum of the NDI aromatic protons of a 0.9×10^{-3} M solution of **1a** in TCE in the presence of C_{60} at different temperatures. (B) Top view of a space filling model of the nanotube, as found in the molecular modeling studies.[47]

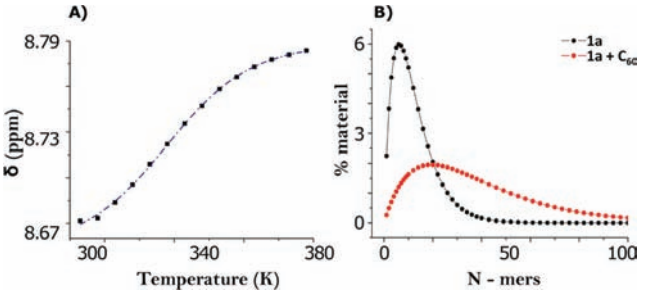

Figure 12. (A) Isodesmic fit of the temperature-dependent shifts of **1a** + C_{60}. (B) Distribution of percentage of material over different nanotube lengths of **1a** (black trace) and **1a** + C_{60} at 273 K (red trace).

cyclohexane in TCE, and then decreases (Figure 10b). The addition of cyclohexane also leads to very slight broadening and blue-shift (~2 nm) of the absorption spectrum (see SI). These observations were paralleled in ^{1}H NMR experiments, leading to the conclusion that the effective hydrogen bond strength is increasing with the concentration of cyclohexane in TCE up to 65%. Above this concentration the change in solute−solvent interactions leads to the destabilization of the nanotube and/or formation of other hydrogen-bonded structures with reduced interaction between the chromophores, causing a decrease in the CD intensity[33] (Figure 10b) and broadening of the ^{1}H NMR signals (see SI).

These solvent-dependent experiments thus highlight the importance of solute−solvent interactions, in addition to COOH hydrogen bonds in the formation of nanotubes. Addition of a noncompeting hydrogen-bonding solvent, such as cyclohexane, increases the effective strength of hydrogen bonds as predicted but at the cost of reduced solute−solvent interactions. This experiment led us to further explore the effect of guests encapsulated within the nanotube cavity primarily by solvophobic interactions, on the stability of the nanotube.

Template Effect of Guests. Our group has previously reported that nanotubes can readily encapsulate C_{60} in chloroform, probably via a solvophobic process, increasing the solubility of C_{60} in this solvent by 16-fold.[2] In our initial report, we were however unsuccessful in the measurement of association constants for the formation of the nanotube and for the formation of host−guest complexes due to the undefined stoichiometry of the interaction and problems arising from the low solubility of C_{60}. Our new approach, using isodesmic fitting of the temperature-dependent ^{1}H NMR chemical shift of NDI aromatic proton in the presence and absence of guests to calculate thermodynamic parameters provides a tool for better understanding of the formation of these host−guest complexes.

The ^{1}H NMR spectrum of **1a** in TCE remains unchanged upon C_{60} complexation, indicating that the nanotubular structure is preserved (CD experiments confirm this observation, see SI). The loss of symmetry of the NDI resonance (see Figure 4a) as a consequence of slow exchange occurs at 303 K for "C_{60} filled" nanotube, 20 °C higher than the "empty" nanotubes in an equally concentrated solution. Presumably the increased stabilization of the nanotube arises from a slowing down of the nanotube dissociation as a result of C_{60}−NDI interaction (Figure 11).

The data obtained from the temperature-dependent ^{1}H NMR of **1a** in the presence of C_{60} could successfully be fitted to an isodesmic model, resulting in $K = (20.9 \pm 0.5) \times 10^3\ M^{-1}$ for the formation of nanotubes at 300 K (Figure 12a). This value is approximately 7 times higher than that obtained for the formation of "empty" **1a** nanotubes, signifying a positive templation and stabilization of the nanotube by C_{60}. The analysis also provided the melting temperature of the "C_{60} filled" nanotube $T_M = 338$ K (19 °C higher than "empty" **1a** nanotubes), the molar enthalpy of "C_{60}-filled" nanotube formation $\Delta H = -87$ kJ mol^{-1} and change in entropy $\Delta S = -205$ J mol^{-1} K^{-1}. The DP_N value at 273 K for a 0.9×10^{-3} M **1a** solution in TCE was calculated as 5.3 for "empty" **1a** nanotube and 15.7 for "C_{60}-filled" **1a** nanotube. A simulation of the exponential distribution of species (vide supra) in a 0.9×10^{-3} M solution with the above DP_N values shows the increase in the length of the nanotube on templation by C_{60} (Figure 12b). C_{60} clearly stabilizes the well-ordered environment shown in Figure 5b due to the good match between the solvophobic surface of guest and the inner walls of the host nanotube. Comparison of the enthalpy and entropy contributions suggests that the increase in enthalpy for the formation of "C_{60}-filled" nanotube results in the formation of more strongly bound nanotubes but at the cost of increased restriction of relative motion as reflected in larger entropic costs, leading to partial entropy−enthalpy compensation (see SI).

^{1}H NMR analysis of "C_{60}-filled" nanotubes of **2** and **3** in TCE also showed positive templation of the nanotube by C_{60}. However, the association constant at 300 K for the formation of "C_{60}-filled" nanotubes for **2** and **3** is only 2 times higher than for "empty" nanotubes compared to the 7 times stabilization achieved in the case of **1a** (see SI). This may be due to enhanced stabilization of the nanotube via van der Waals interactions between the trityl groups of i and i + 3 NDI units in **1a**, as a consequence of formation of tighter nanotubes.

NDI nanotubes can also act as size selective receptors for ammonium ions in chloroform solution.[21] Furthermore, in a competition experiment with C_{60} and ammonium ions, this dynamic system showed a tendency to form mixed complexes in which both guests are present simultaneously in the nanotube cavity, apparently driven by the interaction between ion pair and C_{60}.[22] To further understand this system, we carried out a ^{1}H NMR investigation of **1a** in the presence and absence of ammonium ions in a manner similar to the C_{60} experiments. Isodesmic fit of the temperature-dependent data of **1a** in the presence of tetrabutylammonium chloride ($N^+Bu_4Cl^-$) yielded $K = (1.37 \pm 0.03) \times 10^3\ M^{-1}$ for the formation of nanotubes at 300 K. The analysis also provided the melting temperature of the "ion-pair-filled" nanotube $T_M = 320$ K, the molar enthalpy of nanotube formation $\Delta H = -45$ kJ mol^{-1}, and change in entropy $\Delta S = -89$ J mol^{-1} K^{-1}. The slight reduction of association constant compared to "empty" nanotubes of **1a** may be due to the destabilization

dx.doi.org/10.1021/ja2088647 |J. Am. Chem. Soc. 2012, 134, 566–573

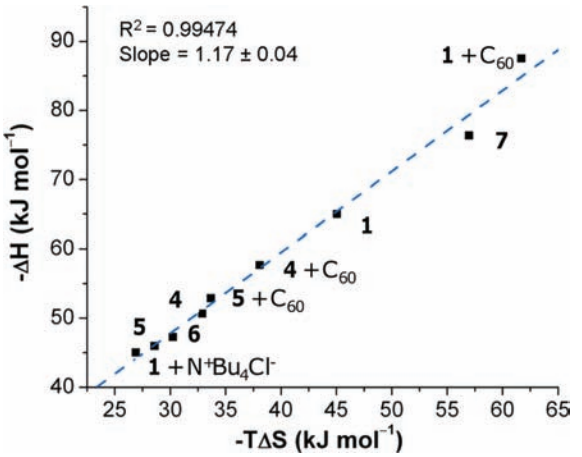

Figure 13. $(-\Delta H)$ vs $(-T\Delta S)$ at 300 K for all the NDI molecules used in this study.

of the hydrogen bonds by the ion pairs, or to the formation of competing non-nanotubular complexes, resulting in the formation of shorter nanotubes which results in the observed increase in entropy.

These results represent a successful extension of the isodesmic model, for the first time, to supramolecular polymerizations templated by the formation of host−guest complexes. The thermodynamic parameters of the host−guest complexes obtained from the fitting were in agreement with results obtained from previously published experiments and enabled a quantitative understanding of their stability. Stabilizing guests such as C_{60} were found to shift the equilibrium of the NDI toward the formation of nanotubes (Figure 2) through favorable solvophobic interactions while destabilizing guests such as $N^+Bu_4Cl^-$ resulted in the increase of nonaggregated monomers.

Summary of Thermodynamic Observations. All the results described above can be summarized graphically in a plot of $-\Delta H$ vs $-T\Delta S$ as shown in Figure 13. A linear correlation is obtained between $-\Delta H$ and $-T\Delta S$, implying that the increase in enthalpy provided by either side chain or host−guest interactions is compensated to a large extent by the increase in entropic penalties due to the formation of tighter nanotubes. As a consequence of this entropy−enthalpy compensation, a substantial increase in ΔG is not observed. This close match between enthalpy and entropy shows the delicate nature of this supramolecular nanotube scaffold.

CONCLUSIONS

By treating the hydrogen-bonded equilibria of the NDI nanotube as a dynamic combinatorial system, we have elucidated its thermodynamics of formation and have shown for the first time how its host−guest interactions can be quantified. We have observed that the formation of the nanotube is best described by an unexpected isodesmic mechanism, rationalized as a consequence of entropy−enthalpy compensation. To the best of our knowledge, the NDI nanotube represents the first synthetic supramolecular polymer where this phenomenon has been observed and analyzed.

The analysis also revealed a significant templation effect by C_{60} on the formation of the nanotube. Encapsulation of C_{60} led to 7-fold increase in the effective association constant for the formation of the nanotube, resulting in the increase of DP_N of nanotube in solution from 5.3 to 15.7 at 273 K. This corresponds to an increase in the effective melting temperature (T_M) by 20 °C.

The investigation of the weak CH···O nonclassical hydrogen-bonds and side chain interactions on the stability of the nanotube gave insights into the limitation of this nanotubular system. Due to the close match between between entropic loss and enthalpic gain, a substantial improvement in ΔG is difficult to achieve. In conclusion, this study illustrates the delicate nature of the NDI nanotube by highlighting the fine balance between entropy and enthalpy that governs its self-assembly process.

ASSOCIATED CONTENT

Supporting Information. Experimental procedures; characterization of **4** and **5**, including their ^1H and ^{13}C NMR spectra; crystallographic data; fitting of isodesmic model and calculation of thermodynamic parameters. This material is available free of charge via the Internet at http://pubs.acs.org.

AUTHOR INFORMATION

Corresponding Author
g.d.pantos@bath.ac.uk; jkms@cam.ac.uk

ACKNOWLEDGMENT

We thank Dr. J. E. Davies for collecting X-ray data, Professor C. A. Hunter, and F. B. L. Cougnon for helpful discussions. We thank EPSRC (J.K.M.S.), Gates Cambridge Trust and St. John's College (N.P.), The Netherlands Organization for Scientific Research−NWO (M.M.J.S.), and Pembroke College, University of Cambridge, and University of Bath (G.D.P.) for funding.

REFERENCES

(1) de Greef, T. F. A.; Smulders, M. M. J.; Wolffs, M.; Schenning, A. P. H. J.; Sijbesma, R. P.; Meijer, E. W. *Chem. Rev.* **2009**, *109*, 5687–5754.
(2) Chen, Z.; Lohr, A.; Saha−Möller, C. R.; Würthner, F. *Chem. Soc. Rev.* **2009**, *38*, 564–584.
(3) Martin, R. B. *Chem. Rev.* **1996**, *96*, 3043–3064.
(4) Zhao, D.; Moore, J. S. *Org. Biomol. Chem.* **2003**, *1*, 3471–3491.
(5) Smulders, M. M. J.; Nieuwenhuizen, M. M. L.; de Greef, T. F. A.; van der Schoot, P.; Schenning, A. P. H. J.; Meijer, E. W. *Chem.—Eur. J.* **2010**, *16*, 362–367.
(6) Oosawa, F.; Kasai, M. *J. Mol. Biol.* **1962**, *4*, 10–21.
(7) Sept, D.; McCammon, J. A. *Biophys. J.* **2001**, *81*, 667–674.
(8) Wegner, A.; Engel, J. *Biophys. Chem.* **1975**, *3*, 215–225.
(9) Flyvbjerg, H.; Jobs, E.; Leibler, S. *Proc. Natl. Acad. Sci. U.S.A.* **1996**, *93*, 5975–5979.
(10) Kaiser, T. E.; Stepanenko, V.; Würthner, F. *J. Am. Chem. Soc.* **2009**, *131*, 6719–6732.
(11) Hill, J. P.; Jin, W.; Kosaka, A.; Fukushima, T.; Ichihara, H.; Shimomura, T.; Ito, K.; Hashizume, T.; Ishii, N.; Aida, T. *Science* **2004**, *304*, 1481–1483.
(12) Jin, W.; Yamamoto, Y.; Fukushima, T.; Ishii, N.; Kim, J.; Kato, K.; Takata, M.; Aida, T. *J. Am. Chem. Soc.* **2008**, *130*, 9434–9440.
(13) Peterca, M.; Percec, V.; Imam, M. R.; Leowanawat, P.; Morimitsu, K.; Heiney, P. A. *J. Am. Chem. Soc.* **2008**, *130*, 14840–14852.
(14) Percec, V.; Imam, M. R.; Peterca, M.; Wilson, D. A.; Heiney, P. A. *J. Am. Chem. Soc.* **2009**, *131*, 1294–1304.
(15) Percec, V.; Dulcey, A. E.; Balagurusamy, V. S. K.; Miura, Y.; Smidrkal, J.; Peterca, M.; Nummelin, S.; Edlund, U.; Hudson, S. D.; Heiney, P. A.; Duan, H.; Magonov, S. N.; Vinogradov, S. A. *Nature* **2004**, *430*, 764–768.

(16) Jonkheijm, P.; van der Schoot, P.; Schenning, A. P. H. J.; Meijer, E. W. *Science* **2006**, *313*, 80–83.
(17) Beljonne, D.; Hennebicq, E.; Daniel, C.; Herz, L. M.; Silva, C.; Scholes, G. D.; Hoeben, F. J. M.; Jonkheijm, P.; Schenning, A. P. H. J.; Meskers, S. C. J.; Phillips, R. T.; Friends, R. H.; Meijer, E. W. *J. Phys. Chem. B* **2005**, *109*, 10594–10604.
(18) Pantoş, G. D.; Pengo, P.; Sanders, J. K. M. *Angew. Chem., Int. Ed.* **2007**, *46*, 194–197.
(19) Pantoş, G. D.; Wietor, J.-L.; Sanders, J. K. M. *Angew. Chem., Int. Ed.* **2007**, *46*, 2238–2240.
(20) Wietor, J.-L.; Pantoş, G. D.; Sanders, J. K. M. *Angew. Chem., Int. Ed.* **2008**, *47*, 2689–2692.
(21) Tamanini, E.; Ponnuswamy, N.; Pantoş, G. D.; Sanders, J. K. M. *Faraday Discuss.* **2010**, *145*, 205–218.
(22) Tamanini, E.; Pantoş, G. D.; Sanders, J. K. M. *Chem.—Eur. J.* **2010**, *16*, 81–84.
(23) Lehn, J. M. *Chem. Soc. Rev.* **2007**, *36*, 151–160.
(24) Corbett, P. T.; Leclaire, L.; Vial, L.; West, K. R.; Weitor, J−L.; Sanders, J. K. M.; Otto, S. *Chem. Rev.* **2006**, *106*, 3652–3711.
(25) Herrmann, A. *Org. Biomol. Chem.* **2009**, *7*, 3195–3204.
(26) Ladame, S. *Org. Biomol. Chem.* **2008**, *6*, 219–226.
(27) Bhosale, S. V.; Jani, C. H.; Langford, S. J. *Chem. Soc. Rev.* **2008**, *37*, 331–342.
(28) Sakai, N.; Mareda, J.; Matile, S. *Chem. Commun.* **2010**, *46*, 4225–4237.
(29) Cubberley, M. S.; Iverson, B. L. *J. Am. Chem. Soc.* **2001**, *123*, 7560–7563.
(30) McConnell, H. M. *J. Chem. Phys.* **1957**, *27*, 226–229.
(31) Hunter, C. A.; Anderson, H. L. *Angew. Chem., Int. Ed.* **2009**, *48*, 7488–7499.
(32) Hunter and Anderson have also shown that this analysis for the ligand−receptor interactions can be extended to the study of self-assembling supramolecular polymers.
(33) Bullheller, B. M.; Pantoş, G. D.; Sanders, J. K. M.; Hirst, J. D. *Phys. Chem. Chem. Phys.* **2009**, *11*, 6060–6065.
(34) A value of $K = (4.3 \pm 0.3) \times 10^2\ M^{-1}$ was obtained at 300 K for reference compound phenylacetic acid (see SI).
(35) Calderone, C. T.; Williams, D. H. *J. Am. Chem. Soc.* **2001**, *123*, 6262–6267.
(36) Dunitz, J. D. *Chem. Biol.* **1995**, *2*, 709–712.
(37) Krishnamurthy, V. M.; Bohall, B. R.; Semetey, V.; Whitesides, G. M. *J. Am. Chem. Soc.* **2006**, *128*, 5802–5812.
(38) Hunter, C. A.; Tomas, S. *Chem. Biol.* **2003**, *10*, 1023–1032.
(39) Williams, D. H.; Stephens, E.; O'Brien, D. P.; Zhou, M. *Angew. Chem., Int. Ed.* **2004**, *43*, 6596–6616.
(40) Williams, D. H.; O'Brien, D. P.; Bardsley, B. *J. Am. Chem. Soc.* **2001**, *123*, 737–738.
(41) Stefankiewicz, A. R.; Tamanini, E.; Pantoş, G. D.; Sanders, J. K. M. *Angew. Chem. Int. Ed* **2011**, *50*, 5725–5728.
(42) Steiner, T *Angew. Chem., Int. Ed.* **2002**, *41*, 48–76.
(43) Ousaka, N.; Sato, T.; Kuroda, R. *J. Am. Chem. Soc.* **2009**, *131*, 3820–3821.
(44) Pengo, P.; Pantoş, G. D.; Otto, S.; Sanders, J. K. M. *J. Org. Chem.* **2006**, *71*, 7063–7066.
(45) Tambara, K.; Ponnuswamy, N.; Hennrich, G.; Pantoş, G. D. *J. Org. Chem.* **2011**, *31* (9), 272–278.
(46) Cook, J. L.; Hunter, C. A.; Low, C. M. R.; Perez-Velasco, A; Vinter, J. G. *Angew. Chem., Int. Ed.* **2007**, *46*, 3706–3709.
(47) AM1 semiempirical level using GAMESS package; the starting geometries for the nanotube and fullerenes were obtained from X-ray data for the free nanotube and the free fullerene and convergence criterion was 0.01 kcal $Å^{-1}$ mol^{-1}.